

See discussions, stats, and author profiles for this publication at: <https://www.researchgate.net/publication/227613917>

Deuterium Isotope Effects in the Combustion of Formulated Nitramine Propellants

ARTICLE *in* PROPELLANTS EXPLOSIVES PYROTECHNICS · FEBRUARY 1994

Impact Factor: 1.6 · DOI: 10.1002/prop.19940190108

CITATIONS

3

READS

32

3 AUTHORS, INCLUDING:



Paul C Trulove

United States Naval Academy

121 PUBLICATIONS **2,448** CITATIONS

SEE PROFILE



Robert D. Chapman

Naval Air Warfare Center Weapons Division

49 PUBLICATIONS **372** CITATIONS

SEE PROFILE



Kinetic Deuterium Isotope Effects in the Combustion of Formulated Nitramine Propellants⁽¹⁾

Paul C. Trulove^(2a), Robert D. Chapman^(2b), and Scott A. Shackelford^(2c)

Fundamental Technologies Division, Phillips Laboratory, Edwards Air Force Base, California 93523 (USA)

Kinetische Deuteriumisotopie-Effekte beim Abbrand von Nitramintreibstoff-Formulierungen

Der kinetische Deuteriumisotopie-Effekt wurde verwendet zur Untersuchung des geschwindigkeitsbestimmenden Vorganges beim Abbrand von Nitramintreibstoff-Formulierungen. Modell-Treibstoffe, die entweder HMX, RDX oder ihre deuterierten Analoge enthielten, wurden zu Kügelchen gepreßt und unter Stickstoffatmosphäre in einer optischen Bombe abgebrannt. Die Größen der beobachteten Isotopie-Effekte zeigten, daß HMX und RDX sichtbaren Einfluß ausüben auf den Abbrand der untersuchten Treibstoffe. Andererseits, unter der Annahme eines übereinstimmenden Mechanismus zwischen Zersetzung und Abbrand, ist es aufgrund der beobachteten Isotopie-Effekte naheliegend, daß das Aufbrechen der CH-Bindung im HMX oder RDX der geschwindigkeitsbestimmende Schritt für den Abbrand der Nitramintreibstoffe ist. Die beobachteten Werte des Isotopie-Effektes für die Treibstoff-Formulierungen HMX-CW5 und RDX-CW5 bei einem Druck von 6,99 MPa waren $1,29 \pm 0,09$ bzw. $1,24 \pm 0,07$ im Vergleich zum theoretischen Wert von 1,29 für einen Primäreffekt beim Bruch der CH-Bindung bei 673 K.

Effets cinétiques d'isotopie de deutérium lors de la combustion de compositions de propergol à base de nitramine

L'effet cinétique d'isotopie de deutérium a été utilisé pour étudier le phénomène limitant la vitesse lors de la combustion de compositions de propergol à base de nitramine. Des compositions modélisées de propergol contenant soit le HMX, le RDX ou leurs analogues deutérés ont été comprimées sous forme de petites billes et brûlées sous pression d'azote dans une bombe optique. Les valeurs des effets d'isotopie observés ont montré que le HMX et le RDX exerçaient une influence décisive sur la combustion des propergols utilisés. D'autre part, en supposant un mécanisme cohérent entre la destruction et la combustion, les effets d'isotopie observés montrent clairement que la rupture de la liaison CH dans le HMX ou le RDX est l'étape qui permet de contrôler la vitesse lors de la combustion du propergol à base de nitramine. Les valeurs observées de l'effet d'isotopie pour les compositions de propergol HMX-CW5 et RDX-CW5 à une pression de 6,99 MPa étaient de $1,29 \pm 0,09$ ou de $1,24 \pm 0,07$ par rapport à la valeur théorique de 1,29 pour un effet primaire lors de la rupture de la liaison CH à 673 K.

Summary

The kinetic deuterium isotope effect was used to investigate the rate-limiting process in the combustion of formulated nitramine propellants. Model propellant formulations containing either octahydro-1,3,5,7-tetranitro-1,3,5,7-tetrazocine (HMX), hexahydro-1,3,5-trinitro-1,3,5-triazine (RDX), or their deuterated analogues were pressed into pellets and burned under nitrogen pressure in a window bomb. The magnitudes of the observed deuterium isotope effects indicate that the HMX and RDX exert significant control over the combustion phenomenon of the propellants studied. Furthermore, assuming a consistent mechanism between decomposition and combustion, the observed isotope effects suggest that a carbon-hydrogen bond rupture in HMX or RDX is the rate-controlling step in the combustion of the model nitramine propellants. Observed isotope effect values for HMX-CW5 and RDX-CW5 formulated propellants at 1000 psig (6.99 MPa) pressure were 1.29 ± 0.09 and 1.24 ± 0.07 , respectively, compared to a theoretical estimate of 1.29 for a primary effect due to C-H bond rupture at 673 K.

1. Introduction

The nitramines HMX and RDX have been employed in solid rocket propellants as replacements for both fuel (e.g., aluminum) and oxidizer (e.g., ammonium nitrate) in an effort to enhance performance and reduce visible exhaust products⁽³⁾. While acceptable performance and reduction of the visible exhaust plume have been achieved, nitramine-

based solid propellants possess several undesirable characteristics which have thus far limited their application.

It is difficult to vary the burn rate of nitramine propellants through modification of the propellant formulation. Techniques developed to modify the burn rate of aluminum-ammonium perchlorate propellants - such as changing ingredient particle size, adding catalysts, varying the amounts of ingredients, etc. - have little effect on the burn rates of nitramine propellants. In essence, nitramine propellants tend to burn over a very narrow range, often referred to as the "burn rate box." Furthermore, the burn rates of nitramine propellants are too slow for many applications.

The effect of pressure on the burn rate (r) of a propellant is given by

$$r = a(p_c)^n \quad (1)$$

where p_c is the pressure inside the combustion chamber, a is an empirical constant, and n is the burn rate pressure exponent⁽⁴⁾. The larger the pressure exponent, the greater the change in propellant burn rate with increasing pressure. Unfortunately, nitramine-based propellants possess certain problems which have thus far limited their application. They tend to have large pressure exponents; often $n > 0.8$. As a consequence, the propellant burn rate and the combustion pressure are very sensitive to each other so that catas-

94-29675



1702

94 9 12 074

This document has been approved for public release and sale; its distribution is unlimited.

trophic pressure increases can occur in a few milliseconds⁽⁴⁾. Finally, nitramine-based propellants are generally more hazardous than aluminum-ammonium perchlorate propellants.

If HMX- and RDX-based propellants are to be used on a broad scale, significant improvements in the burn rate range, pressure exponent, and propellant hazard must be made. These, in turn, necessitate a fundamental understanding of the processes governing the energy release in the combustion of HMX and RDX. Recently, researchers have focused their attentions on determining the rate-limiting reactions in the thermal decomposition and high-pressure combustion of HMX and RDX because it is the rate of the slowest reaction which to a large extent controls the global energy release process.

Kinetic isotope effects provide a powerful technique for the investigation of the rate-controlling reactions in thermochemical processes of energetic materials. Recently, isotope effects have been used to study the thermal decomposition and combustion of HMX and RDX⁽⁵⁻¹¹⁾. The results of these experiments implicate a C-H bond rupture as the global rate-controlling step in these thermochemical events. The isotope effect studies have important implications in the improvement of nitramine-based propellants. However, the relevance of results for pure HMX and RDX is limited because of the possibly significant influence that other propellant ingredients may exert on the chemical mechanism of nitramine propellant combustion.

In a continuation of previous combustion work on HMX⁽⁵⁾ and RDX^(6,7), isotope effects in the combustion of model formulated nitramine propellants are reported here. These results are compared to the results for the combustion of the pure nitramines in order to draw conclusions about the effect of propellant ingredients on the nitramine combustion mechanism. Finally, explanations are offered for the observed isotope effects and their kinetic implications.

2. Background

2.1 Kinetic Deuterium Isotope Effect Theory

Kinetic isotope effects long have been recognized for their potential in the study of reaction rates and mechanisms. Normal substituent effects do not always give a clear understanding of a system due to changes in the potential energy surface and possible mechanistic changes which occur upon going from one substituent to another. The potential energy surface and the reaction mechanisms of molecules differing only by isotopic substitution are essentially the same. This allows kinetic isotope effects to be used to investigate the nature of a single potential energy surface and thus a single transition state⁽¹²⁾.

Isotope effects are categorized as being either primary or secondary. A primary (1°) isotope effect occurs when a bond to the isotopic atom is broken during the rate-limiting step. Secondary (2°) isotope effects are those effects which do not involve the rupture of a bond to the isotopic atom but another one in its immediate vicinity. Primary isotope

effects are generally larger than secondary effects. However, determining whether an observed isotope effect is primary or secondary is not trivial. For single-step reactions, kinetic isotope effects are observed when bonds to an isotopic atom undergo changes upon transition to the activated complex. In the case of multi-step reactions, isotope effects will be seen if bonds to an isotopic atom undergo changes in a slow step of the reaction mechanism.

The following discussion focuses on the isotope effects arising when deuterium is substituted for protium, hereafter referred to as Kinetic Deuterium Isotope Effects (KDIEs). For more detailed information, the reader is directed to literature reviews⁽¹²⁻¹⁹⁾.

According to transition state theory, the rate constant k for a reaction is given by

$$k = \frac{k_B T}{h} \kappa \bar{K} \quad (2)$$

where k_B is Boltzmann's constant, T is temperature, and h is Planck's constant. The transmission coefficient (κ) represents the probability that a given system moving in the direction of the reaction path will in fact pass over the potential energy barrier to the products side⁽¹²⁾. The quantity \bar{K} is the equilibrium constant between the reactants and activated complex. For the hydrogen transfer reaction



it takes the form of

$$\bar{K} = \frac{Q_{AHB}^\ddagger}{Q_{AH} Q_B} \exp \left[-\frac{E_a}{RT} \right] \quad (3)$$

where Q_{AHB}^\ddagger is the quantum mechanical partition function for the activated complex, Q_{AH} and Q_B are the partition functions for the reactants, and R is the universal gas constant [the double dagger (\ddagger) is used to identify quantities associated with the activated complex/transition state]. The activation energy for the reaction (E_a) is simply the difference between the zero point energy of the reactants (E_0) and the zero point energy of the activated complex (E_0^\ddagger). For a comparison of rates of protiated and deuterated species' reactions, the KDIE, k_H/k_D , is expressed as

$$\frac{k_H}{k_D} = \frac{\kappa_H}{\kappa_D} \frac{Q_{AHB}^\ddagger/Q_{AH}}{Q_{ADB}^\ddagger/Q_{AD}} \exp \left[-\frac{[\Delta E_a]_D^H}{RT} \right] \quad (4)$$

The quantity $[\Delta E_a]_D^H$ is merely the difference between the activation energy for the reaction with protium ($E_{a,H}$) and the activation energy for the reaction with deuterium ($E_{a,D}$). There are essentially two parts to Eq. (4), each of which may contribute to the magnitude of the KDIE. The first part is the preexponential; it consists of the ratio of the transmission coefficients and the ratio of the partition functions. Under most circumstances, both of these ratios are very close to unity. As such they are normally not considered when evaluating KDIEs. The second portion of Eq. (4) (involving $[\Delta E_a]_D^H$) is the zero point energy contribution.

of most observed isotope effects. In turn, the size of $[\Delta E_a]_D^H$ depends solely on the changes in zero point energy which occur on going from reactants to activated complex.

The temperature dependence of KDIEs may be understood qualitatively from the Arrhenius relationship incorporated into Eq. (4). The preexponential ratio can be considered to be relatively temperature independent⁽²⁰⁾, whereas the exponential $(-[\Delta E_a]_D^H/RT)$ is obviously temperature dependent. Large KDIEs (with the exception of reactions involving quantum mechanical tunneling)⁽¹⁹⁾ are due almost entirely to zero point energy contributions. As such, KDIEs of this type should exhibit a profound dependence on temperature. In contrast, KDIEs with only minimal zero point energy contribution should change little with temperature.

The maximum values of $[\Delta E_a]_D^H$ occur for reactions with linear symmetrical transition states (i.e., the transition state A---H---B is linear, and the A---H and H---B force constants are equal)^(12-14,21). Consequently, KDIEs for this type of reaction will vary the most with temperature. For example, using Eq. (4) and assuming only zero point energy contributions, a KDIE of 7.0 at 298 K decreases to a value of 3.4 at 473 K. For linear unsymmetrical transition states (i.e., H is closer to A or to B), the values of $[\Delta E_a]_D^H$ are smaller, and consequently the temperature dependences of the KDIEs are less than for the symmetrical case. In the same manner as above, a KDIE for an unsymmetrical case which is 2.0 at 298 K would decrease only to 1.55 at 473 K.

Non-linear transition states have values of $[\Delta E_a]_D^H$ which are very close to zero. As such, the preexponential is the primary source of the KDIE for reactions of this type. Because the preexponential varies little with temperature, KDIEs for reactions with non-linear transition states tend to be temperature independent. In fact, a constant KDIE over temperature ranges greater than 50 degrees is a strong indication of a bent transition state⁽²⁰⁾. When the extrapolation of KDIE is carried out to extremely high temperatures, the exponential portion of Eq. (4) reduces to unity. This leaves only the preexponential to contribute to the KDIE. What this preexponential actually represents is the ratio of partition functions [Eq. (3)], which at high temperature reduces to $v_{HL}^\ddagger/v_{DL}^\ddagger$, the ratio of imaginary frequencies describing the motion along the reaction coordinate^(19,21). At infinite temperature the value of this ratio of imaginary frequencies and thus the value of the KDIE should in theory fall between unity and $(\mu_{DL}^\ddagger/\mu_{HL}^\ddagger)^{1/2}$ (the ratio of the reduced masses along the reaction path)⁽¹⁹⁾. For primary KDIEs in which the isotopic atom is in motion along the reaction path, the infinite mass approximation can be used to give

$$\sqrt{\frac{\mu_{DL}^\ddagger}{\mu_{HL}^\ddagger}} \approx \sqrt{\frac{m_D}{m_H}} \quad (5)$$

where m is the mass of the isotopic atom. Thus, the high temperature limiting value for a primary KDIE should be $(2)^{1/2}$ or 1.41. However, due to unharmonicity and inaccuracies in the infinite mass approximation this value⁽²²⁾ is closer to 1.35.

In secondary KDIEs, the isotopic atom is not involved in motion along the reaction path. Thus, the infinite mass

approximation cannot be used to simplify the ratio of reduced masses $(\mu_{DL}^\ddagger/\mu_{HL}^\ddagger)^{1/2}$. Because of the small size of the isotopic atom and its rather minor contribution to the reduced mass, μ_{DL}^\ddagger is only slightly larger than μ_{HL}^\ddagger , giving a value of $(\mu_{DL}^\ddagger/\mu_{HL}^\ddagger)^{1/2}$ very close to unity. Thus, at infinite temperature, secondary KDIEs approach unity.

In the discussion thus far, attention has been focussed on the KDIE arising from a single isotopic atom. It is frequently the case, however, that reactions are performed on molecules containing more than one isotopic atom. This gives rise to the possibility of compounded isotope effects. Essentially, when there is more than one isotopic atom, the effects of each atom multiply⁽¹²⁾; and it is possible to have a compounded isotope effect wherein one atom contributes a primary effect and one or more atoms contribute a secondary effect. A more comprehensive treatment of isotope effects takes into account such factors.

The determination of whether an isotope effect is primary or secondary is relatively straight-forward for reactions involving a single isotopic atom. If the observed effect is greater than the maximum possible secondary effect, then the KDIE can unambiguously be assigned to a primary effect. If, however, the KDIE is less than the maximum secondary effect, then other information must be used to determine whether the effect is primary or secondary.

2.2 Energetic Material KDIE Studies

Because of the complexity of KDIE theory, approximations have been made in an effort to simplify its application to experimental data. Unfortunately, KDIE theory has frequently been oversimplified to the point where it becomes valid only under idealized circumstances. The resulting application of this simplified model to experimental data has led to frequent errors in the interpretation of KDIE⁽¹³⁾.

Recently, KDIEs have been used to identify the rate-controlling step in HMX and RDX decomposition^(6,9,10) and deflagration⁽⁹⁾ processes as well as in combustion phenomena⁽⁵⁻⁷⁾. Assignment of the type of KDIE (1°, 2°, or inverse) observed during an energetic compound's decomposition process or its combustion phenomenon has been an evolutionary procedure. The inherent complexity of KDIE theory and of these high-energy events themselves^(5,9,23) dictates that approximations must be used when interpreting experimental data. Nevertheless, approximations must also be used cautiously to avoid oversimplifications that could result in conceptual errors⁽¹³⁾. Balancing the necessity of approximation with the potential pitfall of oversimplification was addressed when the KDIE approach was first extended from earlier well defined solvolyzed or gas-phase chemical reactions to condensed-phase thermochemical decomposition processes which consist of numerous sequential and parallel chemical reactions^(14,24). Application of the KDIE approach to the high-pressure combustion regime of a pure energetic compound represents an additional step in complexity of interpretation; both a condensed-phase decomposition process and a gaseous flame oxidation process simultaneously occur, each with its own myriad of chemical reactions⁽⁵⁾. Use of the KDIE approach

with a formulated propellant mixture comprised of several compounds represents the most complex case to date and epitomizes this dilemma where KDIE approximations must be balanced against the pitfall of oversimplification.

Evolution of KDIE interpretation under the complex, high-temperature, high-pressure conditions produced by energetic compound decomposition and deflagration processes plus combustion, thermal explosion, or detonation phenomena began with a mechanistic KDIE study of the thermochemical decomposition exhibited by liquid 2,4,6-trinitrotoluene (TNT) and its deuterium-labeled analogue (TNT- $\alpha,\alpha,\alpha-d_3$)⁽²⁴⁾. Based upon a theoretical high-temperature limit of 1.41 for a 1° KDIE⁽¹⁴⁾, coupled with chemical structures of TNT and its previously reported decomposition products^(25,26), the KDIE value of 1.66 determined from the experimental induction periods was assigned to be a 1° KDIE. This value revealed that the methyl group's C-H bond dissociation constitutes the rate-controlling step in liquid TNT's thermochemical decomposition process. Subsequently, this same criterion of 1.41 as a minimum 1° KDIE value was used in a study of the thermochemical decomposition of solid 1,3,5-triamino-2,4,6-trinitrobenzene (TATB) and its deuterium-labeled analogue (TATB- d_6) to show that a 1.5 KDIE value represented a 1° KDIE, where the amino group's N-H bond dissociation is the rate-controlling step⁽²⁷⁾. This interpretation was supported by the significant reduction of a proton NMR signal in the decomposed residue left at the end of solid TATB's decomposition. A further mechanistic investigation^(9b) conducted on the thermochemical decomposition of HMX and HMX- d_8 used 1.35 as a minimum experimental 1° KDIE value based on precedent theory about limiting values of this parameter^(22,28). Subsequent KDIE studies of HMX and RDX thermochemical decomposition^(6,9,10) and combustion^(5,7) used 1.35 as a 1° KDIE lower limit. Extrapolations of the observed KDIE values to standard temperature (298 K) essentially utilizing Eq. (4) as an approximation yielded in every case normalized room-temperature KDIE values exceeding a suggested minimum 1° KDIE value of 2.5 at standard temperature⁽²⁹⁾.

KDIE studies also have been conducted with thermally initiated thermal explosion⁽²⁷⁾ and shock-initiated detonation^(10,31) phenomena. Thermal explosion studies of TATB and TATB- d_6 produced a critical temperature difference where TATB- d_6 was 12 degrees higher. The $> 10^\circ$ temperature rise suggests a 1° KDIE greater than 2 in the thermally initiated chemical reactions which produce TATB's thermal explosion and suggests that N-H bond rupture could be the rate-controlling step. Interestingly, product analyses by X-ray photoelectron spectroscopy conducted on hot spots produced in mechanical impact sub-initiated thermal explosions of TATB revealed the same type of products formed (furazans and furoxans) as those produced during its thermochemical decomposition⁽³¹⁻³⁵⁾. The same was true in shock sub-initiated detonation studies of TATB samples^(33,34) and lends support to shock-initiated KDIE studies conducted on TNT⁽³⁰⁾, RDX⁽¹⁰⁾, and HMX⁽¹⁰⁾, where small but statistically significant differences between normal and deuterium-labeled compounds were interpreted as coming from the same rate-controlling step as that observed in the

thermochemical decomposition process. Indeed, all products seen in the impact and shock sub-initiated TATB studies resulted from N-H bond rupture, with the furoxans being produced solely by the same N-H bond dissociation seen as the rate-controlling step in TATB's thermochemical decomposition and thermally initiated thermal explosion. In the XPS-analyzed impact sub-initiated RDX and TNT samples, products again were identified which were either the same as those isolated in thermochemical decomposition (where C-H bond dissociation had been identified as the rate-controlling step) or which were formed *only* via dissociations involving C-H bonds. In summary, XPS-identified products formed from TNT, TATB, and RDX in hot spot cavities essentially resulted from the same covalent bond dissociation which produced experimental 1° KDIE values observed in previous thermochemical decomposition, deflagration, combustion, thermal explosion, and detonation studies of these compounds^(8,31-35).

While the assumption of 1.35 as a 1° KDIE minimum value has withstood the test of time to date, a recent *ab initio* molecular orbital calculation conducted on intramolecular decomposition of TNT between 245 K and 269 K⁽³⁶⁾ further illustrates the complex nature of condensed-phase KDIE interpretation. While the calculated 1° KDIE value ranges from 2.4 to 2.5 with tunneling corrections, the lower experimental value (1.66)⁽²⁴⁾ indicates that other factors, including intermolecular reactions^(8a,37-39) and small compounded 2° KDIEs, are present.

Since HMX and RDX are congenerous cyclic nitramines which differ by only one "methylene-nitrimine" unit ($-CH_2N-NO_2$ or $-CD_2N-NO_2$), the possible isotope effects for HMX and RDX are almost identical. For deuterium substitution at the methylene carbon atoms, isotope effects should be observed if either a C-H, C-N, or N-N bond were broken in the rate-limiting process. A C-H bond rupture would result in a compounded primary effect due to a primary contribution from the deuterium in motion along the reaction path and a secondary contribution from the deuterium α to the reaction path (Fig. 1). Estimates of individual primary and secondary effects have been made⁽¹⁴⁾ based on: an observed 2° KDIE of ~ 1.07 for thermolysis of 4-methylene-1-pyrazoline⁽⁴⁰⁾; observed KDIEs of 2.98 (1°) and 1.30 (2°) for elimination reactions at 323 K⁽¹²⁾; and application of Eq. (4) (assuming the preexponential as

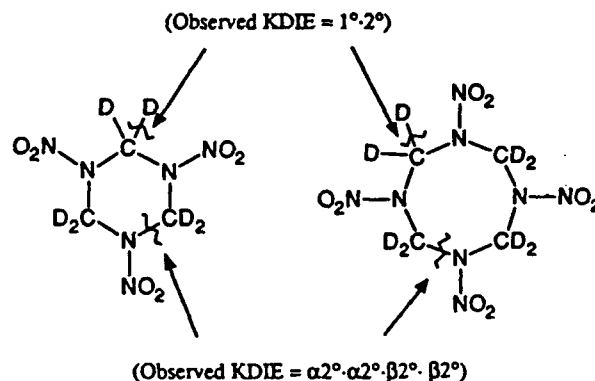


Figure 1. Possible isotope effects in RDX- d_6 and HMX- d_8 .

unity) to extrapolate the latter KDIEs to a temperature yielding an estimated 2° KDIE of 1.07 and a corresponding 1° KDIE of 1.32. Using these values, the estimated magnitude for a KDIE from a C-H bond rupture in HMX and RDX would be $1.32 \cdot 1.07 = 1.41$. In theory, the four deuteriums *gamma* to the reaction site could contribute to the compounded primary effect. However, considering the small magnitude of α -secondary effects under these conditions, the secondary effects of γ -deuteriums can be neglected.

A C-N bond rupture in the rate-limiting process would result in a compounded secondary effect made up of the contributions from the two α -deuteriums and the two β -deuteriums (Fig. 1). Depending on the orientation of the activated complex, the isotopic effects of β -deuteriums (secondary isotope effects of the second kind) can be as large as the effects of α -deuteriums (secondary isotope effects of the first kind). Under most conditions, however, the effects of β -deuteriums are smaller. Assuming this to be the case, an acceptable estimate for the contribution of the β -deuteriums to the compounded secondary KDIE would be 1.02 per deuterium^(12,41,42). Using this estimate and the 2° KDIE approximation above, the estimated magnitude of the effect for a C-N bond rupture would be $1.07 \cdot 1.07 \cdot 1.02 \cdot 1.02 = 1.19$. This value compares very well with that determined in the previous thermochemical decomposition investigation of HMX where the 2° KDIE value ranged from 1.13 to 1.28⁽⁹⁾.

There is sufficient evidence both theoretical⁽⁴³⁾ and experimental^(9,44) to conclude that the N-N bond is the weakest covalent bond in HMX and RDX. Furthermore, these studies indicate that the N-N bond rupture is relatively facile at the temperatures of nitramine decomposition⁽⁴⁵⁾. Consequently, it was concluded that the N-N bond rupture was unlikely to be the *rate-limiting* step.

2.3 KDIE in HMX Decomposition

HMX decomposition, as measured by isothermal differential scanning calorimetry (IDSC), possesses three regimes similar to what is seen in TNT decomposition. The induction phase, the exothermic acceleratory phase, and the decay phase have been attributed to physical states of HMX; solid, mixed melt, and liquid, respectively⁽⁹⁾. The KDIEs for each of these phases are listed in Table 1.

Table 1. Deuterium Isotope Effects in HMX Decomposition

Method	Temp. Range [K]	Physical State	Ratio ^(a)	KDIE	Ref.
IDSC	551-553	solid	t_D/t_H	$2.21 \pm 0.18^{(b)}$	9
IDSC	551	solid	t_D/t_H	$1.74 \pm 0.22^{(c)}$	9
IDSC	551-553	mixed melt	k_H/k_D	$0.85 \pm 0.22^{(b)}$	9
IDSC	551	mixed melt	k_H/k_D	$1.05 \pm 0.19^{(c)}$	9
IDSC	551-553	liquid	k_H/k_D	$1.13 \pm 0.08^{(b)}$	9
IDSC	551	liquid	k_H/k_D	$1.28 \pm 0.21^{(c)}$	9
TGA	508-555	solid and melt	k_H/k_D	$2.06 \pm 0.12^{(b,d)}$	10b
TGA	508-555	solid and melt	t_D/t_H	$1.91 \pm 0.19^{(b)}$	10b

(a) t_i is the induction time for thermochemical decomposition in the IDSC and TGA experiments. (b) HMX and HMX- d_8 were prepared by different methods. (c) HMX and HMX- d_8 were prepared by identical methods. (d) Recalculated from published rate constants.

Thermogravimetric analysis (TGA) has been employed to study isotope effects in HMX decomposition^(10b). Because nitramine decomposition proceeds to gaseous products early on, thermogravimetric analysis, which measures sample weight loss with time, is a practical method for measuring rate constants and thus isotope effects. The KDIE values obtained for HMX decomposition using TGA are also listed in Table 1. An average KDIE of 2.06 ± 0.12 was observed for experiments in the temperature range of 235 °C - 282 °C, comprised of solid-state and then melt phase HMX. By use of the empirical 1.35 criterion⁽⁹⁾, the isotope effect was attributed to a rate-limiting C-H bond rupture. Following the logic used to explain the KDIE in the IDSC induction phase, the isotope effect measured by TGA also appears to be a primary effect compounded by secondary effects.

2.4 KDIE in RDX Decomposition

The KDIE values obtained for RDX decomposition are given in Table 2. The isotope effect values for IDSC and TGA are in the same range even though TGA measured the KDIE for the solid and mixed melt state decomposition while IDSC measured a KDIE for decomposition in the liquid. By use of the 1.35 criterion, all three KDIEs for RDX decomposition were designated as primary^(6,10). Although the TGA value of 1.53 is smaller than the IDSC values, it would still require a relatively large secondary effect from all four deuteriums for it to be the result of a compounded secondary effect. Therefore, as was the case for the HMX induction phase (because it is unlikely that the effects can be due to a compounded secondary effect), the KDIE for RDX decomposition appears to be the result of a rate-controlling C-H bond rupture.

2.5 KDIE in HMX and RDX Combustion

The burn rates of pressed pellets of HMX and HMX- d_8 were measured at three different pressures⁽⁵⁾. The ratio of the burn rates (r_H/r_D), which was assumed to be equivalent to the ratio of rate constants, at each pressure is given in Table 3. By using the 1.35 KDIE criterion, the 1.37 ± 0.22 and 1.60 ± 0.16 KDIE values at 500 psig (3.55 MPa) and 1000 psig (6.99 MPa), respectively, were designated as primary effects. A lower value at 1500 psig (10.44 MPa) of 1.24 ± 0.20 was explained as a consequence of one of three possible causes. HMX combustion proceeds through an

Table 2. Deuterium Isotope Effects in RDX Decomposition

Method	Temp. Range [K]	Physical State	Ratio	KDIE	Ref.
IDSC	500	liquid	k_H/k_D	$1.80^{(a)} \pm 0.18$	6c
IDSC	505	liquid	k_H/k_D	$1.66^{(a)} \pm 0.17$	6c
IDSC	510	liquid	k_H/k_D	$1.54^{(a)}$	6b
IDSC	515	liquid	k_H/k_D	$1.46^{(a)} \pm 0.17$	6c
TGA	472-489	solid and liquid	k_H/k_D	$1.53^{(b,c)} \pm 0.06$	10b

(a) The RDX and RDX- d_6 were prepared by identical methods. (b) The RDX and RDX- d_6 were prepared by different methods. (c) Recalculated from published rate constants.

Table 3. Deuterium Isotope Effects in HMX and RDX Combustion

Compound	Pressure [psig]	KDIE (r_H/r_D) ^(a)	Ref.
HMX	500	1.37 ± 0.22	5
HMX	1000	1.61 ± 0.16	5
HMX	1500	1.24 ± 0.20	5
RDX	500	1.37 ± 0.14	7
RDX	1000	1.47 ± 0.21	7

(a) Reported values are 95 % confidence limits for estimates of the mean KDIE.

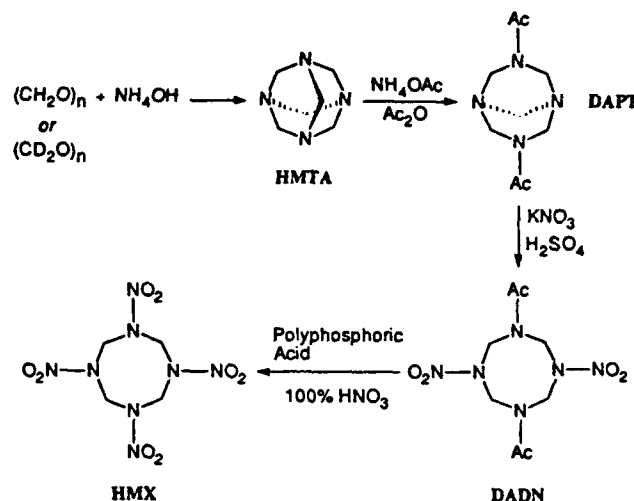
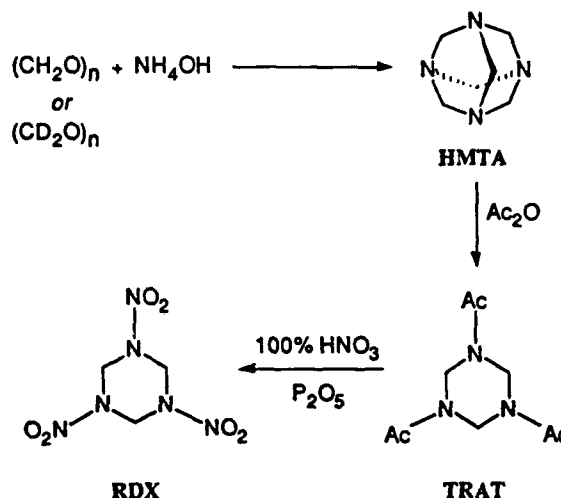
exothermic decomposition producing gaseous products which further react in the flame. The change in the isotope effect with pressure may be attributable to a change in the physical state where a majority of the HMX decomposition occurred. It is possible that as pressure increased, the HMX decomposition went from the solid state to the liquid⁽⁵⁾. It is also possible, however, that the differences between pressures are due to a simple statistical deviation^(1a,5,46). Therefore, a reasonable value for the isotope effects in HMX combustion would be an average of the KDIE for all three pressures (i.e., 1.40 ± 0.11).

The burn rates of pressed pellets of RDX and RDX- d_6 were also measured at 500 psig and 1000 psig (3.54 MPa and 6.99 MPa). The ratios of these burn rates at each pressure are listed in Table 3. By application of the same criteria as were applied to HMX, these effects were designated as primary^(6,7).

3. Experimental

General Procedures. To ensure that differences in experimental results were not due to impurities or sample history, the deuteriated forms of HMX and RDX were synthesized in the same manner as the protiated forms. This was accomplished by substituting paraformaldehyde- d_2 for paraformaldehyde in the synthesis of hexamethylenetetramine to give hexamethylenetetramine- d_{12} . The deuteriated hexamethylenetetramine was then used in the synthesis of either HMX- d_8 or RDX- d_6 . The synthesis of HMX and HMX- d_8 follows a four-step procedure diagramed in Figure 2 and has been described in detail in the literature^(5,47-49). The synthesis of RDX and RDX- d_6 follows a three-step procedure diagramed in Figure 3 and has been described in detail in the literature^(6,50,51).

All chemicals were reagent grade or better and were used without purification. The paraformaldehyde- d_2 was obtained from MSD isotopes. Burdick and Jackson distilled-in-glass acetone was used to convert HMX from the

**Figure 2.** HMX synthesis.**Figure 3.** RDX synthesis.

α - to the β -polymorph. A JEOL FX-90Q 90-MHz FT-NMR was used to obtain all 1H NMR spectra. Melting point data were obtained using a Thomas-Hoover Unimelt capillary melting apparatus and unsealed capillary tubes. All melting points are uncorrected.

The ingredients used in the model propellant formulations were standard propellant grade unless otherwise noted and were obtained from the following manufacturers: dibutyltin diacetate (DBTDA), reagent grade, Alfa Products; hydroxyl-terminated polybutadiene (HTPB, trade name R-45M) Lot #803445, ARCO; isophorone diisocyanate (IPDI)

Lot #6932-0008, Chemische Werke Hüls AG; poly(diethyl-ene glycol adipate), hydroxyl-terminated (trade name R-18) Lot #D-018 4-002, Mobay; trimethylolethane trinitrate (TMETN) Lot #6H-10M, Trojan; triphenylbismuthine (TPB), reagent grade, Aldrich. For certain comparative pressed pellet experiments, propellant grade HMX and RDX were used. The HMX, Lot #78L675-014 and weight median diameter of 26 μm , and the RDX, Lot #77H150-058 and weight median diameter of 35 μm , were obtained from Aerojet.

HMX and RDX Particle Size. The 90 %, 50 %, and 10 % particle diameters and the calculated specific surface area for each of the four synthesized nitramines are listed⁽⁵²⁾ in Table 4. The particle diameter data were obtained using a Malvern 3600E Particle Size Analyzer by a light scattering technique to determine the number of particles in each of a large number of diameter bands. By using these data, the diameters listed in Table 4 were calculated. The data in Table 4 are interpreted as follows: the particle size listed for the 90 % diameter is the diameter below which 90 % of the sample particle diameters fall. The analyzer determines the surface area of each band by using the median diameter of the band and assuming that all particles are perfect spheres. The specific surface area for a sample is simply the sum of the surface areas for all the diameter bands. Because many particle samples do not possess a normal distribution of sizes, it is conceivable that two samples with different particle distributions can have the same specific surface area.

Table 4. Particle Diameters (μm) and Calculated Specific Surface Area (m^2/cm^3)

Compound	90 %	50 %	10 %	Specific Surface Area ⁽⁵²⁾ [m^2/cm^3]
HMX	47.4	21.9	6.2	0.13
HMX- d_8	60.3	35.7	8.6	0.10
RDX	61.2	36.7	11.8	0.10
RDX- d_8	53.7	22.8	8.3	0.11

3.1 Pressed Pellet Preparation

The bottom halves of No. 3 gelatin capsules (Eli Lilly Co.) were used to contain the pressed nitramine powder and to act as an inhibitor to ensure the uniform horizontal burning of the pellets. The pellets were prepared by first placing the gelatin capsule into the pellet die (Figs. 4 and 5) and then filling the capsule with the appropriate nitramine powder. The powder was then lightly compressed to allow for the addition of more nitramine; more powder was added and then compacted. This compacting procedure was repeated several times until the level of the pressed powder was a few millimeters above the top lip of the capsule. A hydraulic press (Model C, Fred S. Carver, Inc.) and a punch [dia. 0.208 in (5.28 mm)], which fit snugly inside the gelatin capsule [I.D. 0.211 in (5.36 mm)], were used to compress the powder to a pressure of 50 psi (340 kPa) on a $1\frac{7}{8}$ -inch (47.6-mm) ram (Fig. 4). The punch was then withdrawn, and more powder was added to a level above the capsule lip. The powder was pressed to its final pressure of

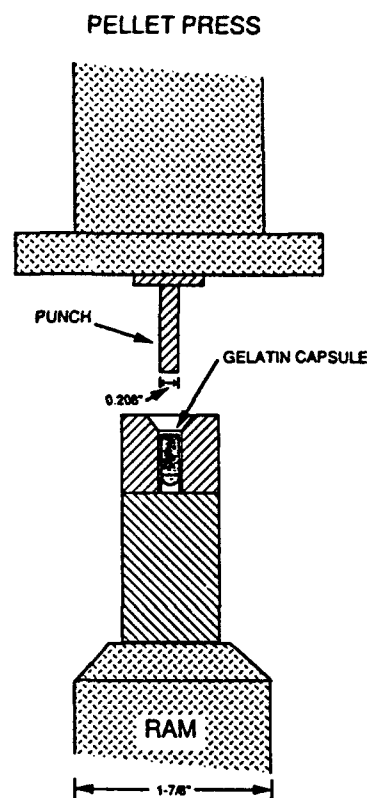


Figure 4. Pellet pressing apparatus.

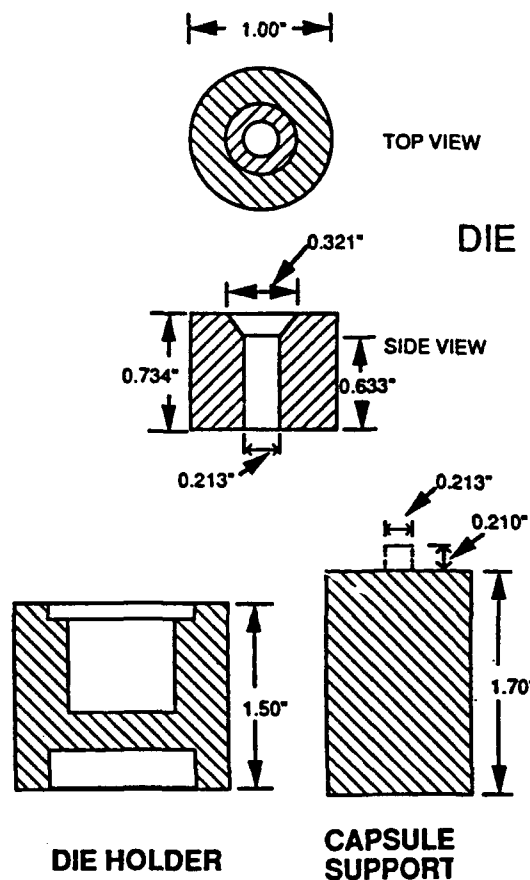


Figure 5. Pellet die, holder, and capsule support.

100 psi (690 kPa) on the 17/8-inch (47.6-mm) ram. This final pressure equates to a pressure on the 0.211-inch (5.36-mm) diameter pellet of 7900 psi (54.5 MPa). The powders were pressed to this pressure in order to give pellet densities approximately the same as the densities of the formulated propellants.

The pellet was removed by placing the die with capsule onto the die holder (Fig. 5) and pressing the capsule out the bottom of the die with the punch. A razor blade was used to shave off the excess powder down to the top lip of the gelatin casing. The densities of the RDX, RDX-*d*₆, HMX, and HMX-*d*₈ pellets are listed in Table 5 along with the densities of the propellant pellets. After pressing, the pellets were approximately 13 mm x 5.4 mm in size.

Table 5. Pellet Densities for the Pressed Powders and the Formulated Propellants^(a)

Pellet Material	Density [g/cm ³] ^(b)
HMX/HMX- <i>d</i> ₈	1.525 ± 0.015
RDX/RDX- <i>d</i> ₆	1.400 ± 0.010
HMX/HMX- <i>d</i> ₈ CW5	1.616 ± 0.015
RDX/RDX- <i>d</i> ₆ CW5	1.480 ± 0.030
HMX/HMX- <i>d</i> ₈ PB	1.507 ± 0.016
RDX/RDX- <i>d</i> ₆ PB	1.395 ± 0.025

(a) Compositions of formulations are given in Table 6.

(b) The reported error is at the 95 % confidence level.

3.2 Model Propellant Preparation

Propellant Formulations. The nitramine propellant formulations used in this study, designated CW5 and PB, are listed in Table 6. The CW5 formulation (Table 6a) was chosen because of its simplicity and because it contained both an energetic plasticizer and a high oxygen content polymer. The CW5 formulation is a relatively energetic nitramine propellant which burns very uniformly owing to an almost equal balance between fuel and oxidizer components.

The PB propellant formulation (Table 6b) was also chosen for its simplicity. In addition, it has been used previously in studies involving both combustion modeling⁽⁵³⁾ and propellant burning properties⁽⁵⁴⁾. Thus, a large amount of

information exists dealing with the PB propellant burning characteristics. The PB propellant is much less energetic than the CW5 propellant. It has a fuel-rich formulation which burns in a very heterogeneous manner giving off a great deal of carbonaceous residue. The CW5 and PB propellants represent the opposite extremes with respect to energetics and burning properties; they should therefore provide a relevant test of isotope effects in cured nitramine propellants.

Propellant Binders. In our experiments two different types of binders were used. The binder of the CW5 formulation employed a polyester polymer (R-18) which was 37 % by weight oxygen and had a number average molecular weight (M_n) of 1400. The CW5 formulation also employed a nitrate ester plasticizer, trimethylolethane trinitrate (TMETN), which increased the energy of the binder in addition to increasing binder elasticity. The PB formulation used a polybutadiene polymer (R-45M), which was 3.6 % by weight oxygen with a number average molecular weight (M_n) of 2800. Because the PB formulations did not contain a plasticizer, their binder was much harder than that in the CW5 formulation.

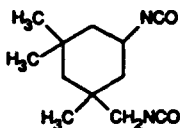
Both polymers were crosslinked using a urethane cure. This involves the condensation reaction of the isocyanate curative with the hydroxyl end group on the polymer to form a urethane linkage. The cure catalyst appears to facilitate the curing process by stabilizing the alcohol-isocyanate complex, thus enhancing the rate of formation of the urethane linkages⁽⁵⁵⁾.

The propellants were prepared on a 2.5-g scale in a 50-ml Teflon beaker. Initially, the polymer, curative, and, if necessary, plasticizer were mixed into a viscous homogeneous liquid. The nitramine, which had been dried at 60 °C for 12 h, was then mixed in until a smooth, pasty consistency was achieved. Finally, the cure catalyst was added and the completed propellant carefully packed into the bottom halves of five No. 3 gelatin capsules. Great care was taken to avoid leaving any trapped air in the propellant. Large-scale propellant mixing operations can avoid the problem of trapped gases by performing most propellant mixing proce-

Table 6a. CW5 Propellant Formulation

Compound	Structure	Percent [wt]
Nitramine		73.20
R-18 (polymer)		8.51
TMETN (plasticizer)		16.89
IPDI (curative)		1.39
DBTDA (cure catalyst)	$(CH_3CH_2CH_2CH_2)_2Sn(OCOCH_3)_2$	0.01

Table 6b. PB Propellant Formulation

Compound	Structure	Percent [wt]
Nitramine		80.00
R-45M (polymer)	$\text{HO}-\left[\text{CH}_2\text{CH}=\text{CHCH}_2 \right]_{m-1} \left(\text{CH}_2\text{CH}_2 \right)_n \left[\text{CH}_2\text{CH}=\text{CHCH}_2 \right]_{m-1} \text{OH}$ $\text{CH}=\text{CH}_2$	18.52
IPDI (curative)		1.46
TPB (cure catalyst)	$(\text{C}_6\text{H}_5)_3\text{BI}$	0.02

dures under a vacuum. However, because it is impractical if not impossible to use normal mixing methods on a 2.5-g scale, our initial propellant mixtures were prepared and cured at atmospheric pressure. Not unexpectedly, these propellants contained trapped gases in the form of bubbles in the propellant. When pellets of these propellants were placed inside the window bomb and then pressurized to 1000 psig, the sides of the pellets were contracted due to the compression of the bubbles inside the cured propellant. This problem was avoided if the propellant was cured under pressure: the propellant-filled capsules were cured at 40 °C in a pressure bomb (Parr Model 1108 Oxygen Bomb) pressurized to 50 atm (735 psia, 5.07 MPa) with nitrogen. The increased curing pressure either forced out or compressed the bubbles in the propellant. The CW5 propellants were fully cured after 12 h at 40 °C. However, the PB propellants required from 24 h to 36 h at 40 °C to cure fully. The densities of the propellants are listed in Table 5. The cured CW5 and PB propellant pellets were approximately 13.5 mm x 5.4 mm in size.

PVC Coated Propellants. The gelatin capsules frequently cracked due to dehydration when propellant curing required more than 24 h. Because the propellant burning surface propagated down these cracks, making accurate burn rate determination extremely difficult, the damaged gelatin capsules did not function effectively as burning inhibitors. Therefore, several experiments were performed using a polyvinyl chloride (PVC) coating as the burning inhibitor. This was accomplished by first preparing the propellant in the gelatin capsules as described above. The fully cured encapsulated propellants were then placed in a dilute aqueous acetic acid solution to dissolve away the gelatin. The propellant pellets were then thoroughly washed with distilled water and air-dried. The pellets were dipped into a dilute solution of PVC in dichloromethane and air-dried. Finally, a razor blade was used to shave off a small disk of propellant from the top of the pellet to give an uncoated surface for burning.

3.3 Window Bomb Combustion Procedure

Burn rate experiments were performed in a reinforced concrete test cell at the Air Force Astronautics Laboratory

(Phillips Laboratory, Air Force Systems Material), Propellant Experimental Area 1 - 30. All experiments were monitored remotely from a control room adjacent to the test cell.

Window Bomb. The window bomb (AFRPL Window Bomb drawing #X7616176) used for all combustion experiments is shown in Figure 6. Samples in the window bomb were illuminated using a xenon spot light (Color Arc 2000). Experiments were recorded using a high-speed video system (Ektapro 1000, Kodak-Spin Physics). Data were collected at a rate of 1000 frames per second with timing data recorded on each video frame.

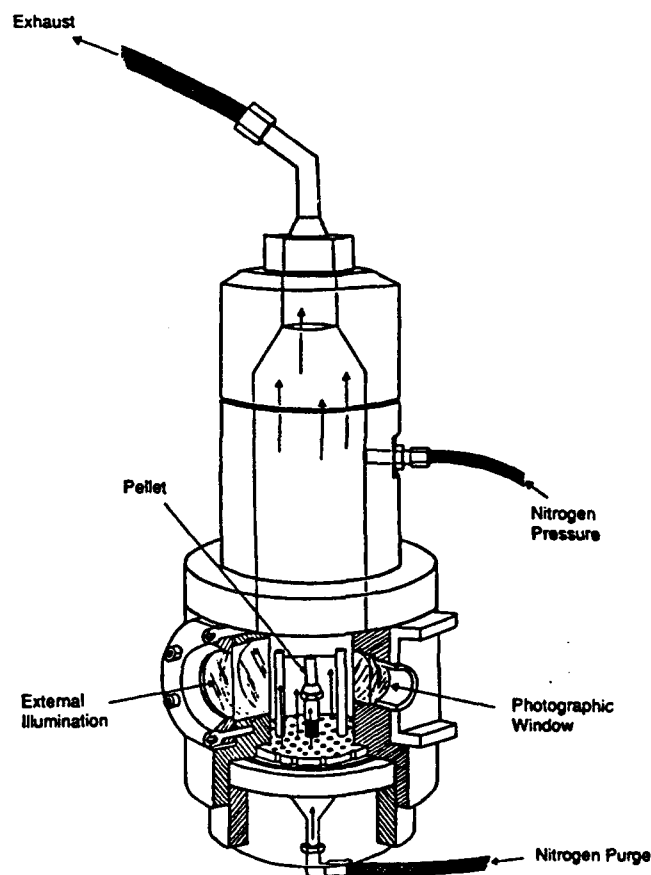


Figure 6. High pressure window bomb.

Burn Rate Experiments. A typical burn rate experiment began by first placing a ruler on the base of the window bomb in the same location as occupied by the pellet (Fig. 7A). The base was then screwed on to the bomb and approximately one hundred frames of the scale were taken using the high-speed video system. These data were later used to determine burn rates. The scale was then removed and replaced with a pellet placed atop of a small piece of putty (Fig. 7B). The pellet, with a Nichrome wire stretched across the top, and the base were then attached to the bomb. Normally the window bomb was pressurized to 1000 psig (6.99 MPa) with nitrogen prior to the experiment. The pressure inside the window bomb was regulated to ± 10 psi (0.07 MPa) during the experiment. A constant 15 psid [15-psi (0.10 MPa) differential between inlet and exit pressures] nitrogen purge during the experiment maintained a clear photographic path to the pellet by removing combustion products and dissipating convective heat currents. The pellet was ignited by the Nichrome wire and the burning recorded using the high-speed video system.

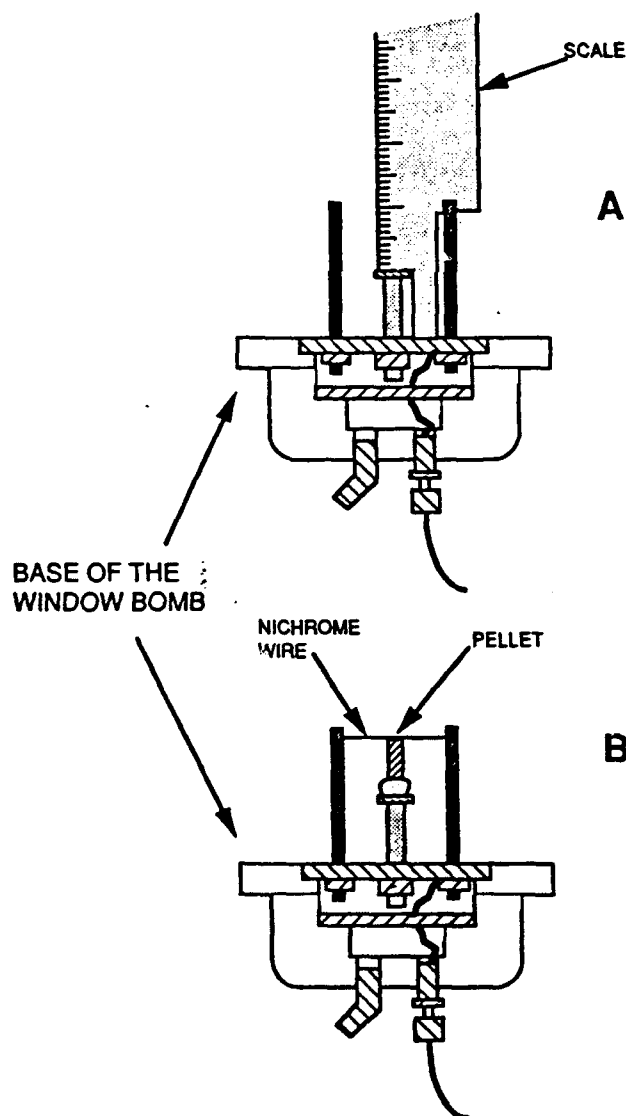


Figure 7. Placement of pellet and scale.

Burn rates were determined in the following manner. A single video frame of the ruler inside the window bomb was displayed on a video monitor. A clear Mylar sheet, containing a grid which exactly matched the ruler markings displayed on the monitor, was taped to the screen. The video of the pellet burn was then advanced until all the effects of ignition had dissipated. This was normally after about the top 20 % of the pellet had burned. At this point the time given on the video frame and the distance on the grid were recorded. The video was then advanced until the pellet burn reached the point where the curvature of the pellet bottom began. At this location the time and distance were again recorded. The pellet burn rate was calculated by taking the distance burned over the change in time.

4. Results and Discussion

The linear burn rate of nitramines and nitramine propellants depends on both kinetic and physical parameters^(4,54). In our experiments, factors such as pressure, temperature, the shape and size of the burning surface, etc. are essentially the same for two samples differing only by isotopic substitution. Thus, any burn rate differences should be due to the effect of isotopic substitution on the rate-limiting process in the combustion mechanism. Because it is currently impractical if not impossible to obtain kinetic rate constants of individual reactions from combustion experiments, burn rates must be used to obtain isotope effect values. The relationship between burn rate and kinetic rate constants of the combustion phenomenon's reactions permits the determination of a rate-limiting step from KDIE values⁽⁵⁾.

Nitramine and nitramine propellant combustion begins with condensed phase decomposition reactions at the burning surface and proceeds through to gas phase oxidation reactions in the luminous flame^(4,5,56). Reaction temperatures for combustion range from approximately 673 K at the burning surface to in excess of 1800 K in the luminous flame⁽⁵⁴⁾. A fundamental principle of reaction kinetics is that reaction rates increase with increasing temperature. In addition, it can be shown that reaction rates tend to increase when going from a non-mobile condensed phase to the gas phase⁽⁵⁷⁾. Thus, it would seem that the slowest reactions in the combustion mechanism occur in the condensed phase^(5,58). The numerous mechanistic models proposed for HMX and RDX condensed-phase decomposition suggest a limited number of reactions occurring in the condensed phase due to the early production of gas-phase intermediates^(9,59-67). Recent theoretical studies indicate that after the early bond-breaking steps of HMX and RDX decomposition, the further breakup of the nitramine becomes relatively facile⁽⁴³⁾. From this, one can reasonably conclude that it is likely that the slowest step in the chemically controlled nitramine combustion mechanism occurs early in the condensed-phase nitramine decomposition.

Depending on the initial conditions, the decompositions of HMX and RDX follow either a first order (Eq. 6)^(6,10,68-71) or an autocatalytic rate law (Eq. 7)^(9,70b,72).

$$\frac{d\alpha}{dt} = k(1-\alpha) \quad (6)$$

$$\frac{d\alpha}{dt} = k\alpha(1-\alpha) \quad (7)$$

The extent of reaction is represented by α , t is time, and k is the kinetic rate constant for the reaction. It can be shown that

$$\frac{d\alpha}{dt} = rC \quad (8)$$

where r is the linear burn rate and C is a shape factor which depends on the dimensions of the burning surface⁽⁷³⁾. Assuming that the same process which controls the rate of decomposition also controls the rate of combustion, then with respect to the equations above [Eqs. (6) - (8)], the linear burn rate should be proportional to the kinetic rate constant such that KDIE values can be obtained from burn rates by assuming

$$\frac{r_H}{r_D} = \frac{k_H}{k_D} \quad (9)$$

The rate constant k for the combustion reaction is dependent on the rate constant of the slowest step and to a lesser extent on the steps preceding the slow step⁽⁷⁴⁾. Since the rate-controlling process for nitramine combustion appears to occur early in the decomposition, the value of k should reflect primarily the rate constant of the slow step. Thus, the KDIE values obtained from burn rates should be reasonably representative of the effect of deuterium substitution on the rate-controlling process.

Results from some computational modeling of nitramine propellant burn rates suggest that k is proportional to r^2 instead of r ^(53,75-80). If k is in fact proportional to r^2 , this would mean that the true KDIE values for the nitramine and nitramine propellant combustion reaction rate constants would be even larger than the values described here (viz., the square of the KDIEs based on r). The assumption of proportionality to r rather than r^2 allows the most conservative estimation of KDIEs consistent with current combustion theories. Ultimately, either approach would not significantly affect the conclusions drawn here.

4.1 Burn Rate Experiments

In the following experiments the relative burn rate differences between samples containing either the protiated or deuteriated nitramine are measured. Additionally, it was our purpose to compare the KDIEs of the pure nitramines with the KDIEs of the corresponding propellant mixtures. Toward this end, every effort was made to preclude differences in burn rate due to synthesis, sample history, propellant mixing, pellet preparation, and pellet density.

Pressed Pellet Results

As a baseline for future comparison to model nitramine propellants we repeated combustion studies^(5,6) on HMX, HMX- d_8 , RDX, and RDX- d_6 pressed pellets, acquiring the burn rate data listed in Table 7. The burn rates of commercial grade HMX and RDX pressed pellets were also measured, giving values of 0.535 ± 0.057 in/s (13.6 ± 1.4 mm/s) and 0.551 ± 0.020 in/s (14.0 ± 0.5 mm/s), respectively. These burn rates are in the same range as the values listed for the synthesized HMX and RDX, indicating that the results given in Table 7 are reasonable.

The KDIE of 1.40 ± 0.11 for HMX combustion at varying pressures (500 psig - 1500 psig) reported previously⁽⁵⁾ is consistent with the 95 % confidence interval of 1.30 ± 0.05 for the mean isotope effect for HMX determined here. The previous report of 1.47 ± 0.21 for RDX^(6,7) under conditions identical to these (1000 psig) is also consistent with our experimental value of 1.31 ± 0.04 for pure RDX (Table 7).

Using the evaluation criteria developed in the Background, the estimate for the isotope effect arising from a C-H bond rupture in HMX or RDX is 1.41. The estimated isotope effect for a C-N bond rupture is 1.19 (also see Background). These estimates were made from data collected at temperatures around 500 K^(1d), whereas the temperature of the burning surface during combustion is approximately 673 K. If one used Eq. (4) and assumed that the isotope effects were due strictly to zero point energy differences (i.e., $[\Delta E_0]_D^H$), then a temperature extrapolation can be performed on the above estimates, giving KDIE values of 1.29 for a C-H bond rupture and 1.14 for a C-N bond rupture at 673 K.

The rate-limiting step for the thermal decomposition of pure HMX and RDX under most conditions appears to be a

Table 7. Burn Rate Results for HMX, HMX- d_8 , RDX, and RDX- d_6 Pressed Pellets at 1000 psig^(a)

HMX r_H [in/s]	HMX- d_8 r_D [in/s]	RDX r_H [in/s]	RDX- d_6 r_D [in/s]
0.503	0.394	0.600	0.449
0.505	0.386	0.587	0.456
0.531	0.395	0.609	0.457
0.503	0.397	0.578	0.452
$\bar{r}_H = 0.510 \pm 0.022$	$\bar{r}_D = 0.393 \pm 0.008$	$\bar{r}_H = 0.594 \pm 0.022$	$\bar{r}_D = 0.454 \pm 0.006$

$$\text{KDIE} = \left(\frac{\bar{r}_H}{\bar{r}_D} \right) = 1.30 \pm 0.05$$

$$\text{KDIE} = \left(\frac{\bar{r}_H}{\bar{r}_D} \right) = 1.31 \pm 0.04$$

^(a) Reported error is at the 95 % confidence level.

C-H bond rupture^(6,9,10). Assuming a consistent rate-limiting process for both decomposition and combustion, and applying the above KDIE criteria for 673 K, the isotope effect values for both HMX and RDX of 1.30 ± 0.05 and 1.31 ± 0.04 , respectively, indicate a rate-limiting C-H bond rupture in the combustion process. These assignments are in agreement with previous HMX and RDX combustion studies⁽⁵⁻⁷⁾.

Effects of Curing Conditions and Burning Inhibitors

The effects of curing conditions and burning inhibitors on propellant burn rate were investigated in order to test the ruggedness of our CW5 propellant formulation. The results of these experiments on CW5 propellant formulations containing commercial grade HMX and RDX are listed in Table 8.

Table 8. The Effects of Burning Inhibitor, Curing, and Curing Pressure on CW5 Propellant Burn Rates at 1000 psig

Formulation	Cure Conditions ^(a)	Burning Inhibitor	Burn Rate [in/s] ^(b)
HMX-CW5	1 atm	Gelatin Capsule	0.175 ± 0.006
HMX-CW5	50 atm	Gelatin Capsule	0.166 ± 0.003
HMX-CW5	uncured ^(c)	Gelatin Capsule	0.158 ± 0.007
HMX-CW5	50 atm	PVC	0.177 ± 0.004
RDX-CW5	1 atm	Gelatin Capsule	0.177 ± 0.003
RDX-CW5	50 atm	Gelatin Capsule	0.178 ± 0.005
RDX-CW5	uncured ^(c)	Gelatin Capsule	0.174 ± 0.004
RDX-CW5	50 atm	PVC	0.186 ± 0.009

^(a) All propellants were maintained at 40 °C until fully cured.

^(b) Reported error is at the 95 % confidence level. ^(c) No DBTDA cure catalyst was added to these propellants.

Our initial propellant mixtures were prepared and cured at atmospheric pressure, but these propellants contained trapped gases in the form of bubbles in the propellant. When pellets of these propellants were placed inside the window bomb and then pressurized to 1000 psig, the sides of the pellets were contracted due to the compression of the bubbles inside the cured propellant. This problem was avoided if the propellant was cured at 50 atm (735 psia, 5.07 MPa). Evidently, the increased curing pressure either forced out or compressed the bubbles in the propellant. As can be seen from the data in Table 8, the effect of the change in curing pressure is very small. There was only a slight decrease in the HMX-CW5 burn rate and no change in the RDX-CW5 burn rate when changing the cure pressure from 1 atm to 50 atm.

The difference in the burn rate of cured versus uncured HMX-CW5 is relatively small. In the case of the RDX-CW5 propellant, the difference is insignificant. These results indicate the relative unimportance of the physical structure of the propellant binder in determining burn rate under the conditions of this study. Consequently, any differences in crosslinking density, and thus binder physical properties, between chemically identical propellant mixes should not introduce any significant variation in burn rate.

There was a small increase in the burn rate of both HMX- and RDX-CW5 propellants when the burning inhibitor was switched from a gelatin capsule to PVC. These differences are most likely due to the different physical

characteristics of the inhibitors. The gelatin capsule was better at limiting the propellant burning to the top surface of the pellet. The PVC coating allowed the propellant burning to proceed down the side of the pellet slightly ahead of the advancing top surface; this allowed more burning surface, thus increasing the overall linear burn rate.

Overall, it can be seen from the data in Table 8 that the variation in parameters had only a minor effect on the CW5 propellant burn rate. Thus, one can conclude that any changes in burn rate between normal and deuterium-labeled propellants should be due strictly to the effect of deuterium on the rate-controlling process.

KDIE in CW5 Propellant Mixtures

The burn rate results for normal and deuterium-labeled HMX- and RDX-CW5 propellants in gelatin capsules are listed in Tables 9 and 10, respectively. Because of the small

Table 9. Burn Rate Results for HMX and HMX-*d*₈ CW5 Propellants at 1000 psig^(a)

HMX-CW5	r_H [in/s]	HMX- <i>d</i> ₈ -CW5 r_D [in/s]
0.173	0.180	0.142
0.174	0.179	0.141
0.178	0.201	0.131
0.159	0.155	0.137
0.162	0.206	0.136
$\bar{r}_H = 0.177 \pm 0.012$		$\bar{r}_D = 0.137 \pm 0.005$

$$KDIE = \left(\frac{\bar{r}_H}{\bar{r}_D} \right) = 1.29 \pm 0.09$$

^(a) Reported error is at the 95 % confidence level.

magnitude of the KDIE for data set I and the low burn rate of the RDX-CW5 propellant compared to the burn rate of the commercial grade RDX-CW5 (Table 7), a second set of data was obtained. The burn rates for both the RDX-CW5 and RDX-*d*₆-CW5 propellants in the second data set were significantly greater than in the first data set. The propellants for the second data set were mixed on a day of higher humidity, and the presence of moisture evidently caused the propellant to degas more than usual. This is the apparent cause of the higher overall burn rates.

It is important to note that each data set is self-consistent. In each data set both the RDX-CW5 and RDX-*d*₆-CW5 propellants were prepared under identical conditions using the same ingredients, the cured pellets were burned on the same day under identical conditions, and the data were reduced in the same manner. Therefore, any differences in burn rates between the RDX-CW5 and RDX-*d*₆-CW5 propellants are due strictly to the effect of deuterium substitution on the rate-limiting process. Consequently, the differences in the KDIE values for the two data sets represent simple statistical variations.

The data in Tables 9 and 10 clearly demonstrate an isotope effect for both HMX- and RDX-CW5 propellant mixtures. The magnitude of the KDIE for HMX-CW5 of 1.29 ± 0.09 is almost identical to that of the pure HMX. The KDIE for RDX-CW5 of 1.24 ± 0.07 is statistically not significant-

Table 10. Burn Rate Results for RDX and RDX-*d*₆ CW5 Propellants at 1000 psig^(a)

Set I		Set II			
RDX-CW5 r_H [in/s]	RDX- d_6 -CW5 r_D [in/s]	RDX-CW5 r_H [in/s]		RDX- d_6 -CW5 r_D [in/s]	
0.162	0.125	0.241	0.253	0.193	0.179
0.164	0.135	0.229	0.218	0.196	0.188
0.143	0.135	0.252	0.245	0.191	0.188
0.156	0.136	0.227	0.238	0.173	0.184
0.156	0.140	0.257			
$\bar{r}_H = 0.156 \pm 0.010$	$\bar{r}_D = 0.134 \pm 0.007$	$\bar{r}_H = 0.240 \pm 0.010$		$\bar{r}_D = 0.187 \pm 0.006$	
KDIE = $\left(\frac{\bar{r}_H}{\bar{r}_D} \right) = 1.16 \pm 0.08$		KDIE = $\left(\frac{\bar{r}_H}{\bar{r}_D} \right) = 1.29 \pm 0.06$			
Average KDIE ^(b) = 1.24 ± 0.07					

(a) Reported error is at the 95 % confidence level. (b) Weighted average for data sets I and II (based on statistical degrees of freedom).

Table 11. Burn Rate Results for HMX, HMX-*d*₈, RDX and RDX-*d*₆ PB Propellants at 1000 psig^(a,b)

HMX-PB r_H [in/s]	HMX- <i>d</i> ₈ -PB r_D [in/s]	RDX-PB r_H [in/s]	RDX- <i>d</i> ₆ -PB r_D [in/s]
0.124	0.104	0.193	0.169
0.109	0.114	0.189	0.156
0.112	0.110	0.195	0.160
0.116	0.107		0.157
0.111	0.110		0.162
$\bar{r}_H = 0.114 \pm 0.007$	$\bar{r}_D = 0.109 \pm 0.005$	$\bar{r}_H = 0.192 \pm 0.008$	$\bar{r}_D = 0.161 \pm 0.006$
$KDIE = \left(\frac{\bar{r}_H}{\bar{r}_D} \right) = 1.05 \pm 0.07$		$KDIE = \left(\frac{\bar{r}_H}{\bar{r}_D} \right) = 1.20 \pm 0.05$	

(a) Reported error is at the 95 % confidence level. (b) PVC was used as the burning inhibitor for all pellets.

ly different at the 95 % confidence level from the value of pure RDX of 1.31 ± 0.04 . These data provide evidence that the chemical mechanism which kinetically controls the combustion of the pure HMX and RDX continues to control the combustion of the HMX and RDX-CW5 propellants. Therefore, a C-H bond rupture during the condensed phase decomposition appears to be the rate-controlling process in the combustion of both HMX- and RDX-CW5 propellant mixtures.

KDIE in PB Propellant Mixtures

The burn rate results for normal and deuterium-labeled HMX- and RDX-PB propellant mixtures are listed in Table 11. The burn rates of PB propellants containing commercial grade HMX and RDX were measured, giving mean values of 0.155 ± 0.007 in/s (3.94 ± 0.18 mm/s) and 0.177 ± 0.006 in/s (4.50 ± 0.15 mm/s), respectively. The commercial grades' results appear to confirm the significantly lower HMX-PB burn rate compared to the RDX-PB and to previous model propellant burn rates.

The KDIE of 1.20 ± 0.05 for the RDX-PB propellant mixture is statistically different at the 95 % confidence level from the KDIE value of 1.31 ± 0.04 for pure RDX. This decrease in isotope effect could be due to many factors. Unlike the CW5 propellant mixtures, the PB propel-

lants burn in a very heterogeneous manner, producing large amounts of carbonaceous residue. This residue tends to remain on the surface of the burning propellant, possibly causing an increase in the burning surface temperature due to increased heat feedback from the flame to the burning surface. This increase in the local temperature of the surface at which the RDX decomposition takes place would be expected to result in a smaller KDIE value. The decrease in the magnitude of the KDIE also could be the result of a change in the RDX decomposition mechanism. This change might be a new rate-limiting step other than C-H bond rupture (e.g., C-N), or it may be the introduction of a competitive rate-limiting feature in addition to the C-H bond rupture. Finally, the difference in KDIE values may simply be due to a statistically inaccurate estimate of the RDX-PB propellant isotope effect value caused by a small sample size.

The RDX-PB KDIE of 1.20 falls between the primary and secondary estimates of 1.29 and 1.14, respectively, at 673 K; thus, it is difficult to assign this effect to either a C-H or a C-N bond rupture. Because of the fact that all previous RDX decomposition and combustion studies indicate a rate-limiting C-H bond rupture and the fact that the KDIE is larger than the estimated secondary effect, the KDIE for the combustion of RDX-PB propellants still could be due to a rate-limiting C-H bond rupture, with other unknown

factors contributing to the observed lower KDIE. However, the assignment is not definitive.

The overall linear burn rates for the HMX-PB propellant as shown in Table 11 are significantly less than for the RDX-PB propellant and all the CW5 propellant mixes. Furthermore, the HMX-PB propellant exhibits a KDIE of only 1.05 ± 0.07 , which is much smaller than for all the other propellants in this study. These data indicate a significant change in overall combustion mechanism between pure HMX and the HMX-PB propellant. Although the isotope effect appears to be real and its value falls well below the estimated secondary effect value, one cannot absolutely rule out the possibility that the observed effect is simply a very small primary effect. Again, unknown factors including physical effects may have become predominant in HMX-PB combustion. Thus, from the available data, it is impossible to make a definitive assignment of a rate-limiting process for HMX-PB propellant combustion.

Interestingly, the "mixed melt" region of HMX decomposition observed previously⁽⁹⁾ also exhibited an isotope effect very close to unity. One could speculate that the small KDIE value for the HMX-PB propellant was due to the majority of HMX decomposition occurring in the mixed melt as opposed to either the solid or liquid phase. This in turn could be the result of the heterogeneous nature of the PB propellant burning. Increased heat feedback caused by the carbonaceous residue formed in HMX-PB combustion could lead to a higher temperature, contributing further to the transition to the "mixed melt" phase.

While assignment of either a 1° or 2° KDIE to a value near 1.35 is not a simple task even with pure compounds, a mixture of compounds like that in a propellant formulation represents an even greater problem. The chemical reactions occurring between all of the chemical compounds during propellant combustion are extremely complex and not well understood to date. This is vividly illustrated in the reasonably simple mixture comprised of 2 % HMX-*d*₈ + 98 % HMX prepared by coprecipitation, which displays an unexpected 29 % - 38 % burn rate reduction at 500 psig (3.55 MPa) and 1000 psig (6.99 MPa)⁽⁵⁾. Past burn rate studies also have shown that simply mixing a binder with a nitramine (HMX or RDX) drastically alters the observed burn rate^(58,81), as does the binder's chemical composition⁽⁵⁴⁾ and its percentage in the propellant formulation⁽⁵⁶⁾. The overall burn rate of the formulated propellant must result from a synergistic interaction where all pure chemical ingredients combine to burn at nearly, but perhaps not exactly, the same rate. Recent FTIR analyses of quenched samples of burning propellant have revealed a slight enrichment of polymeric binder or its decomposed product at the surface⁽⁸²⁾. Interestingly, the inclusion of a binder with a nitramine produces a burn rate lower than that of the pure nitramine^(58,81); even an HMX/GAP formulation displays a lower burn rate than that of the pure HMX or the even higher burn rate exhibited by pure cured GAP samples⁽⁸¹⁾.

While these burn rate characteristics may seem puzzling, the KDIE results from this formulated propellant investigation suggest two factors that may contribute to this observed burn rate behavior. First, a formulated pro-

pellant's burn rate may be determined by rate-controlling steps to which both the deuterium-labeled nitramine and the unlabelled binder contribute in a weighted proportion. The observed KDIE could result from one ingredient's larger KDIE (produced by the labeled nitramine) diluted or reduced by some extent to which the unlabeled binder's "KDIE" value (1.00) is involved. Because both chemical compounds burn at nearly the same rate in the formulated propellant, the rate-controlling step for each pure component must proceed at a rate similar enough to affect the overall KDIE observed as burn rate differences. In a preliminary, simplified conceptual illustration, the following relationship may apply:

$$\alpha \cdot (\text{KDIE})_{\text{HMX}} + \beta \cdot (\text{KDIE})_{\text{binder}} = (\text{KDIE})_{\text{obsd}} \quad (10)$$

where $\alpha + \beta \equiv 1$. The values of α and β could be determined by the chemical composition or structure of the binder and by the amount of binder used in the formulation. This second factor is illustrated by the large difference in the experimentally observed KDIE between the CW5 propellants (where a 1° KDIE assignment undoubtedly is valid if the observed KDIE is a result of a reduction by the R-18 binder's participation) and the PB (R-45M) propellants (where a much smaller KDIE is seen). Whether this difference in observed KDIEs between the R-18 polyester and R-45M HTPB binder results mainly from their difference in chemical structure or from the percentage used relative to the deuterium-labeled nitramine (weight ratios: R-18/nitramine = $8.51/73.20 = 0.16$, and R-45M/nitramine = $18.52/80.00 = 0.23$) cannot be determined without a systematic burn rate study wherein one of the two appropriate variables (chemical structure and binder percentage) is held constant. Future work could address this point.

5. Conclusion

Our research has confirmed the presence of significant isotope effects in the combustion of HMX and RDX. More importantly, we have demonstrated the existence of significant KDIEs during the combustion of model formulated nitramine propellants, confirming the significance of chemical kinetic control in the observed burn rate. The consistency between the effects of the pure nitramines and those of the HMX- and RDX-CW5 and RDX-PB propellants indicates similar rate-controlling processes. The KDIEs observed for the pure nitramines and the above propellants appear to be the result of a rate-controlling C-H bond rupture in the condensed phase. The combustion of the HMX-PB propellant shows an isotope effect value significantly less than that of the pure nitramine, indicating a considerable change in the rate-controlling process.

This report is particularly significant in extending previous findings from pure oxidizers to more realistic propellant systems containing additional ingredients which could complicate the combustion mechanism. In spite of these ingredients' participation in the global combustion mechanism, evidence has been given that in most cases the chemical kinetics of the nitramine ingredient control the global burn rate of the model propellant.

6. References and Notes

- (1) Presented in preliminary form in the following sources:
 - (a) P.C. Trulove, R.D. Chapman, and S.A. Shackelford, "Deuterium Isotope Effects in the Combustion of Formulated Nitramine Propellants", *24th JANNAF Combustion Meeting*, Monterey, CA, 7 October 1987; *CPIA Publ.* 476 (Vol. I), 303-308 (1987).
 - (b) S.A. Shackelford, P.C. Trulove, R.D. Chapman, and R.N. Rogers, "Deuterium Isotope Effects During the Nitramine Combustion Event: Possible Implications to Chemical Kinetics/Mechanisms and Predictive Modeling", *1st JANNAF Combustion Subcommittee Panel on "Kinetic and Related Aspects of Propellant Combustion Chemistry"*, Laurel, MD, 2-4 May 1988; *CPIA Publ.* 503, 115 (1988).
 - (c) S.A. Shackelford, P.C. Trulove, and R.D. Chapman, "Deuterium Isotope Effects in Combustion and Explosion: Impact of Chemical Mechanism and Physical State on Energy Release", *19th Annual International ICT Conference*, Karlsruhe, 29 June - 1 July 1988; [Proc.] 40/1-40/14 (1988).
 - (d) P.C. Trulove, "Kinetic Deuterium Isotope Effects in the Combustion of Nitramine Propellants", Report AFAL-TR-88-072 (1988), Air Force Astronautics Laboratory, Edwards AFB, CA, USA.
- (2) Current addresses of co-authors: (a) Electrochemistry Division, F.J. Seiler Research Laboratory (AFSC), USAF Academy, CO 80840-6528 (USA); (b) TPL, Inc., 3768-B Hawkins St. NE, Albuquerque, NM 87109 (USA); (c) Alliance Pharmaceutical Corp., 3040 Science Park Rd, San Diego CA 9212 (USA).
- (3) W. Klöhn and S. Eisele, "Nitramine Solid Rocket Propellants with Reduced Signature", *Propellants, Explos., Pyrotech.* 12, 71-77 (1987).
- (4) G.P. Sutton and D.M. Ross, "Rocket Propulsion Elements", John Wiley, New York 1976, Ch. 10-12.
- (5) S.A. Shackelford, B.B. Goshgarian, R.D. Chapman, R.E. Askins, D.A. Flanigan, and R.N. Rogers, "Deuterium Isotope Effects during HMX Combustion: Chemical Kinetic Burn Rate Control Mechanism Verified", *Propellants, Explos., Pyrotech.* 14, 93-102 (1989).
- (6) (a) S.A. Shackelford, S.L. Rodgers, and M.B. Coolidge, "Deuterium Isotope Effects in RDX Decomposition and Combustion Process: A Progress Report", *21st JANNAF Combustion Meeting*, Laurel, MD, October 1984; *CPIA Publ.* 412 (Vol. II), 615-621. (b) S.L. Rodgers, W.J. Lauderdale, S.A. Shackelford, W.C. Hurley, and M.B. Coolidge, "Initial Thermochemical Decomposition Mechanisms of Energetic Ingredients", Report AFAL-TR-88-100 (1988), Air Force Astronautics Laboratory, Edwards AFB, CA, USA. (c) S.L. Rodgers, M.B. Coolidge, W.J. Lauderdale, and S.A. Shackelford, "Comparative Mechanistic Thermochemical Decomposition Analyses of Liquid Hexahydro-1,3,5-Trinitro-1,3,5-Triazine (RDX) Using the Kinetic Deuterium Isotope Effect Approach", *Thermochim. Acta* 177, 151-168 (1991).
- (7) S.A. Shackelford, S.L. Rodgers, and R.E. Askins, "Deuterium Isotope Effects During RDX Combustion: Mechanistic Burn Rate-Controlling Step Determination", *Propellants, Explos., Pyrotech.* 16, 279-286 (1991).
- (8) (a) S.A. Shackelford, "Mechanistic Investigations of Condensed Phase Energetic Material Decomposition Processes Using the Kinetic Deuterium Isotope Effect", in: S.N. Bulusu (ed), "Chemistry and Physics of Energetic Materials", Kluwer, Dordrecht 1990, pp. 413-432. (b) S.A. Shackelford, "Mechanistic Relationships of the Decomposition Process to Combustion and Explosion Events from Kinetic Deuterium Isotope Effect Investigations", in: S.N. Bulusu (ed), "Chemistry and Physics of Energetic Materials", Kluwer, Dordrecht 1990, pp. 433-456. (c) S.A. Shackelford, "Condensed Phase Kinetic Deuterium Isotope Effects in High Energy Phenomena: Mechanistic Investigations and Relationships", FJSRL-TR-89-0010 (1989), F.J. Seiler Research Laboratory, USAF Academy, CO, USA.
- (9) (a) S.A. Shackelford, M.B. Coolidge, B.B. Goshgarian, R.N. Rogers, J.L. Janney, and M.H. Ebinger, D.A. Flanigan and R.E. Askins, "Deuterium Isotope Effects in HMX Thermochemical Mechanisms: Decomposition, Deflagration, and Combustion", *20th JANNAF Combustion Meeting*, Monterey, CA, 17-20 October 1983; *CPIA Publ.* 383 (Vol. I), 571-580 (1983). (b) S.A. Shackelford, M.B. Coolidge, B.B. Goshgarian, B.A. Loving, R.N. Rogers, J.L. Janney, and M.H. Ebinger, "Deuterium Isotope Effects in Condensed-Phase Thermochemical Decomposition Reactions of Octahydro-1,3,5,7-Tetranitro-1,3,5,7-Tetrazocine", *J. Phys. Chem.* 89, 3118-3126 (1985).
- (10) (a) S. Bulusu, J.R. Autera, D.A. Anderson, and R.W. Velicky, "Deuterium Kinetic Isotope Effect: An Experimental Probe for the Molecular Process Governing the Initiation of TNT and RDX", *1984 Army Science Conference*, June 1984; [Proc.] (Vol. I), 93-106 (1984). (b) S. Bulusu, D.I. Weinstein, J.R. Autera, and R.W. Velicky, "Deuterium Kinetic Isotope Effect in the Thermal Decomposition of 1,3,5-Trinitro-1,3,5-Triazacyclohexane and 1,3,5,7-Tetranitro-1,3,5,7-Tetrazacyclooctane", *J. Phys. Chem.* 90, 4121-4126 (1986).
- (11) S.A. Shackelford, "Physical State Dependence and Mechanistic Relationships Between Decomposition and Combustion", *AFOSR/ONR Contractors' Meeting on "Combustion, Propulsion, Diagnostics of Reacting Flow"*, Ann Arbor, MI, 19-23 June 1989; AFOSR-TR-90-0833 (1989), pp. 97-101, Air Force Office of Scientific Research, Bolling AFB, DC, USA.
- (12) E.K. Thornton and E.R. Thornton, "Origin and Interpretation of Isotope Effects", in: C.J. Collins, N.S. Bowman (eds), "Isotope Effects in Chemical Reactions", Van Nostrand-Reinhold, New York 1970, Ch. 4.
- (13) F.H. Westheimer, "The Magnitude of the Primary Kinetic Isotope Effect for Compounds of Hydrogen and Deuterium", *Chem. Rev.* 61, 265-273 (1961).
- (14) J. Bigeleisen and M. Wolfsberg, "Theoretical and Experimental Aspects of Isotope Effects in Chemical Kinetics", *Adv. Chem. Phys.* 1, 15-76 (1958).
- (15) J. Bigeleisen, "Chemistry of Isotopes", *Science* 147, 463-471 (1965).
- (16) W.H. Saunders Jr., "Kinetic Isotope Effects", *Surv. Prog. Chem.* 3, 109-146 (1966).
- (17) M.J. Goldstein, "Kinetic Isotope Effects and Organic Reaction Mechanisms", *Science* 154, 1616-1621 (1966).
- (18) R.E. Weston Jr., "Transition-State Models and Hydrogen-Isotope Effects", *Science* 158, 332-342 (1967).
- (19) W.A. Van Hook, "Kinetic Isotope Effects: Introduction and Discussion of the Theory", in: C.J. Collins, N.S. Bowman (eds), "Isotope Effects in Chemical Reactions", Van Nostrand-Reinhold, New York 1970, Ch. 1.
- (20) H. Kwart, "Temperature Dependence of the Primary Kinetic Hydrogen Isotope Effect as a Mechanistic Criterion", *Acc. Chem. Res.* 15, 401-408 (1982).
- (21) T.H. Lowry and K.S. Richardson, "Mechanism and Theory in Organic Chemistry", 3rd ed., Harper & Row, New York 1981, pp. 105-111, 120-123.
- (22) A. Streitwieser, R.H. Lagow, R.C. Fahey, and S. Suzuki, "Kinetic Isotope Effects in the Acetolyses of Deuterated Cyclopentyl Tosylates", *J. Am. Chem. Soc.* 80, 2326-2332 (1958).
- (23) C.E.H. Bawn, "The Decomposition of Organic Solids", in: W.E. Garner (ed), "Chemistry of the Solid State", Academic Press, New York 1955, Ch. 10.
- (24) S.A. Shackelford, J.W. Beckmann, and J.S. Wilkes, "Deuterium Isotope Effects in the Thermochemical Decomposition of Liquid 2,4,6-Trinitrotoluene: Application to Mechanistic Studies Using Isothermal Differential Scanning Calorimetry Analysis", *J. Org. Chem.* 42, 4201-4206 (1977).
- (25) R.N. Rogers, "Combined Pyrolysis and Thin Layer Chromatography: A Method for the Study of Decomposition Mechanisms", *Anal. Chem.* 39, 730-733 (1967).
- (26) J.C. Dacons, H.G. Adolph, and M.J. Kamlet, "Some Novel Observations Concerning the Thermal Decomposition of 2,4,6-Trinitrotoluene", *J. Phys. Chem.* 74, 3035-3040 (1970).
- (27) R.N. Rogers, J.L. Janney, and M.H. Ebinger, "Kinetic Isotope Effects in Thermal Explosions", *Thermochim. Acta* 59, 287-298 (1982).
- (28) G. Herzberg, "Molecular Spectra and Molecular Structure" (Vol. II), Van Nostrand, New York 1950, p. 217.

- (29) G.W. Klumpp, "Reactivity in Organic Chemistry", L. Birladeanu (transl), Wiley, New York 1982, p. 262.
- (30) S. Bulusu and J.R. Autera, "Initiation Mechanism of TNT: Deuterium Isotope Effect as an Experimental Probe", *J. Energetic Mater. J.*, 133-140 (1983).
- (31) J. Sharma, W.L. Garrett, F.J. Owens, and V.L. Vogel, "X-Ray Photoelectron Study of 1,3,5-Triamino-2,4,6-Trinitrobenzene", *J. Phys. Chem.* 86, 1657-1661 (1982).
- (32) J. Sharma, J.C. Hoffsommer, D.J. Glover, C.S. Coffey, F. Santiago, A. Stolovy, and S. Yasuda, "Comparative Study of Molecular Fragmentation in Sub-Initiated TATB Caused by Impact, UV, Heat, and Electron Beams", in: J.R. Asay, R.A. Graham, and G.K. Straub (eds), "Shock Waves in Condensed Matter", Elsevier 1984, pp. 543-546.
- (33) J. Sharma, J.W. Forbes, C.S. Coffey, and T.P. Liddiard, "The Physical and Chemical Nature of Sensitization Centers Left from Hot Spots Caused in Triaminotrinitrobenzene by Shock and Impact", *J. Phys. Chem.* 91, 5139-5144 (1987).
- (34) J. Sharma, J.C. Hoffsommer, D.J. Glover, C.S. Coffey, J.W. Forbes, T.P. Liddiard, W.L. Elban, and F. Santiago, "Sub-Ignition Reactions at Molecular Levels in Explosives Subjected to Impact and Underwater Shock", 8th International Symposium on Detonation, Albuquerque, 15-19 July 1985; NSWC MP-86-194 (1987), pp. 725-733, Naval Surface Warfare Center, Silver Spring, MD, USA.
- (35) J. Sharma, J.W. Forbes, C.S. Coffey, and T.P. Liddiard, "The Nature of Reaction Sites and Sensitization Centers in TATB and TNT", in: S.C. Schmidt and N.C. Holmes (eds), "Shock Waves in Condensed Matter", Elsevier 1988, pp. 565-568.
- (36) J.R. Cox and I.H. Hiller, "Ab Initio Studies of the Decomposition of Energetic Materials. I. Hydrogen Transfer in TNT and in Model Systems", *Chem. Phys.* 124, 39-46 (1988).
- (37) J.T. Swanson, L.P. Davis, R.C. Dorey, and W.R. Carper, "An EPR Study of the Thermal Decomposition of 2,4,6-Trinitrotoluene and its Isotopic Analogues", *Magn. Reson. Chem.* 24, 762-767 (1986).
- (38) J.M. McKinney, L.F. Warren, I.B. Goldberg, and J.T. Swanson, "EPR Observation of Nitroxide Free Radicals During Thermal Decomposition of 2,4,6-Trinitrotoluene and Related Compounds", *J. Phys. Chem.* 90, 1008-1011 (1986).
- (39) J.A. Menapace and J.E. Marlin, "Photochemical Decomposition of Energetic Materials: Observation of Aryl Benzyloxy Nitroxide and Aryl Benzyl Nitroxide Radicals in Solutions of 1,3,5-Trinitrobenzene and Toluene and their Deuterated Analogues at 200 K", *J. Phys. Chem.* 94, 1906-1914 (1990).
- (40) M.H. Chang and R.J. Crawford, "Secondary Deuterium Isotope Effects on Both Rate and Product Determining Steps in the Thermolysis of 4-Methylene-1-Pyrazoline", *Can. J. Chem.* 59, 2556-2567 (1981).
- (41) D.E. Sunko and S. Boric, "Secondary Deuterium Isotope Effects and Neighboring Group Participation", in: C.J. Collins, N.S. Bowman (eds), "Isotope Effects in Chemical Reactions", Van Nostrand-Reinhold, New York 1970, Ch. 3.
- (42) E.A. Halevi, "Secondary Isotope Effects", *Prog. Phys. Org. Chem.* 1, 109-221 (1963).
- (43) (a) C.F. Melius and J.S. Binkley, "The Thermochemistry of Nitramines Using the BAC-MP4 Method", *Workshop on Combustion Probes for Solid Nitramines*, Livermore, CA, 9-11 June 1986; [Rept.] pp. 224-241, U.S. Army Research Office, Research Triangle Park, NC, USA.
- (b) C.F. Melius and J.S. Binkley, "Thermochemistry of the Decomposition of Nitramines in the Gas Phase", 21st Symp. (Int.) Combust., [Proc.] 953-963 (1986).
- (44) R.A. Fifer, "Chemistry of Nitrate Ester and Nitramine Propellants", *Prog. Astronaut. Aeronaut.* 90, 177-237 (1984).
- (45) B. Suryanarayana, R.J. Graybush, and J.R. Autera, "Thermal Degradation of Secondary Nitramines: A Nitrogen-15 Tracer Study of HMX (1,3,5,7-Tetranitro-1,3,5,7-Tetrazacyclooctane)", *Chem. Ind. (London)* 2177-2178 (1967).
- (46) The dependence on pressure of magnitudes of isotope effects is relatively slight at high pressures (> 1 atm) even for gas-phase reactions [R.E. Weston Jr., "Effect of Pressure on the Isotope Effect in a Unimolecular Gaseous Reaction: Tritium and Carbon-13 Effects in the Isomerization of Cyclopropane", *J. Chem. Phys.* 26, 975-983 (1957)]. This dependence for condensed-phase reactions should be even less, so the variations with pressure observed previously⁽⁹⁾ are likely statistical fluctuations.
- (47) V.I. Siele, M. Warman, and E.E. Gilbert, "The Preparation of 3,7-Diacyl-1,3,5,7-Tetraazabicyclo[3.3.1]nonanes", *J. Heterocycl. Chem.* 11, 237-239 (1974).
- (48) M.D. Coburn and D.G. Ott, "A Convenient Synthesis of Nitrogen-15- and Deuterium-Labeled Octahydro-1,3,5,7-Tetranitro-1,3,5,7-Tetrazocine (HMX)", *J. Labelled Compds. Radiopharm.* 18, 1423-1427 (1980).
- (49) V.I. Siele, M. Warman, J. Leccacorvi, R.W. Hutchinson, R. Motto, E.E. Gilbert, T.M. Benzinger, M.D. Coburn, R.K. Rohwer, and R.K. Davey, "Alternative Procedures for Preparing HMX", *Propellants, Explos., Pyrotech.* 6, 67-73 (1981).
- (50) E.E. Gilbert, J.R. Leccacorvi, and M. Warman, "The Preparation of RDX", *ACS Symp. Ser.* 22 (Ind. Lab. Nitrations), 327-340 (1976).
- (51) C.D. Bedford, B.D. Deas, M.M. Broussard, and M.A. Geigel, "Preparation and Purification of Multigram Quantities of TAX and SEX", Report AD-A122816 (1982), SRI International, Menlo Park, CA, USA; *Chem. Abstr.* 99, 73150 (1983).
- (52) K.G. Chandler (Astronautics Laboratory, Edwards Air Force Base, CA), personal communication (1987). The effect of particle size on the burn rate of HMX-CW5 propellant was studied. It was shown that a change in HMX particle size from 20 μ m to 100 μ m increases the propellant burn rate by only 5 %.
- (53) M.W. Beckstead and K.P. McCarthy, "Modeling Calculations for HMX Composite Propellants", *AIAA J.* 20, 106-115 (1982).
- (54) N. Kubota, "Physicochemical Process of HMX Propellant Combustion", 19th Symp. (Int.) Combust., [Proc.] 777-785 (1982).
- (55) G. Huynh-Ba and R. Jerome, "Catalysis of Isocyanate Reactions with Protonic Substrates", *ACS Symp. Ser.* 172 (Urethane Chem. Appl.), 205-217 (1981).
- (56) N. Kubota, "Combustion Mechanisms of Nitramine Composite Propellants", 18th Symp. (Int.) Combust., [Proc.] 187-194 (1981).
- (57) (a) R.P. Wayne, "The Theory of the Kinetics of Elementary Gas Phase Reactions", in: C.H. Bamford and C.F.H. Tipper (eds), "Comprehensive Chemical Kinetics", Elsevier, New York 1969, Vol. 2, Ch. 3. (b) R.A. Fifer, "A Hypothesis for the Phase Dependence of the Decomposition Rate Constants of Propellant Molecules", *Joint ONR, AFOSR, ARO Workshop: "Fundamental Directions for Energetic Material Decomposition Research"*, Berkeley, CA, 20-22 January 1981, Office of Naval Research, Arlington, VA, USA.
- (58) Y. Yano and N. Kubota, "Combustion of HMX-CMDB Propellants (II)", *Propellants, Explos., Pyrotech.* 11, 1-5 (1986).
- (59) M.A. Schroeder, "Critical Analysis of Nitramine Decomposition Results: Some Comments on Chemical Mechanisms", 16th JANNAF Combustion Meeting, Monterey, CA, September 1979; *CPIA Publ.* 308 (Vol. II), 17-34 (1979).
- (60) M.A. Schroeder, "Critical Analysis of Nitramine Decomposition Data: Product Distributions from HMX and RDX Decompositions", 18th JANNAF Combustion Meeting, Pasadena, CA, October 1981; *CPIA Publ.* 347 (Vol. II), 395-413 (1981).
- (61) M.A. Schroeder, "Critical Analysis of Nitramine Decomposition Data: Update, Some Comments on Pressure and Temperature Effects, and Wrap-Up Discussion of Chemical Mechanisms", 21st JANNAF Combustion Meeting, Laurel, MD, October 1984; *CPIA Publ.* 412 (Vol. II), 595-614 (1984).
- (62) Y. Oyumi and T.B. Brill, "Thermal Decomposition of Energetic Materials 22. The Contrasting Effects of Pressure on the High-Rate Thermolysis of 34 Energetic Compounds", *Combust. Flame* 68, 209-216 (1987).
- (63) Y. Oyumi and T.B. Brill, "Thermal Decomposition of Energetic Materials 3. A High-Rate, In-Situ FTIR Study of the Thermolysis of RDX and HMX with Pressure and Heating Rates as Variables", *Combust. Flame* 62, 213-224 (1985).
- (64) R. Behrens, Jr., "Thermal Decomposition of HMX and RDX: Decomposition Processes and Mechanisms Based on STMBMS and TOF Velocity-Spectra Measurements", in: S.N. Bulusu (ed),

- "Chemistry and Physics of Energetic Materials", Kluwer, Dordrecht 1990, pp. 347-368.
- (65) R. Behrens, Jr., "Thermal Decomposition of Energetic Materials: Temporal Behaviors of the Rates of Formation of the Gaseous Pyrolysis Products from Condensed-Phase Decomposition of Octahydro-1,3,5,7-Tetranitro-1,3,5,7-Tetrazocine", *J. Phys. Chem.* 94, 6706-6718 (1990).
- (66) R. Behrens, Jr., "Identification of Octahydro-1,3,5,7-Tetranitro-1,3,5,7-Tetrazocine (HMX) Pyrolysis Products by Simultaneous Thermogravimetric Modulated Beam Mass Spectrometry and Time-of-Flight Velocity-Spectra Measurements", *Intl. J. Chem. Kinet.* 22, 135-157 (1990).
- (67) R. Behrens, Jr., "Determination of the Rates of Formation of Gaseous Products from the Pyrolysis of Octahydro-1,3,5,7-Tetranitro-1,3,5,7-Tetrazocine (HMX) by Simultaneous Thermogravimetric Modulated Beam Mass Spectrometry", *Intl. J. Chem. Kinet.* 22, 159-173 (1990).
- (68) R.N. Rogers, "Simplified Determination of Rate Constants by Scanning Calorimetry", *Anal. Chem.* 44, 1336-1337 (1972).
- (69) R.N. Rogers, "Determination of Condensed-Phase Kinetics Constants", *Thermochim. Acta* 9, 444-446 (1974).
- (70) (a) G.J. Piermarini, S. Block, and P.J. Miller, "Effects of Pressure on the Thermal Decomposition and Chemical Reactivity of HMX, RDX and Nitromethane", *19th Annual International ICT Conference*, Karlsruhe, 29 June - 1 July 1988; [Proc.] 15/1-15/11 (1988).
(b) G.J. Piermarini, S. Block, and P.J. Miller, "Effects of Pressure on the Thermal Decomposition Rates, Chemical Reactivity and Phase Behavior of HMX, RDX and Nitromethane", in: S.N. Bulusu (ed), "Chemistry and Physics of Energetic Materials", Kluwer, Dordrecht 1990, pp. 391-412.
- (71) G.J. Piermarini, S. Block, and P.J. Miller, "Effects of Pressure and Temperature on the Thermal Decomposition Rate and Reaction Mechanism of β -Octahydro-1,3,5,7-Tetranitro-1,3,5,7-Tetrazocine", *J. Phys. Chem.* 91, 3872-3878 (1987).
- (72) P.J. Miller, S. Block, and G.J. Piermarini, "Effects of Pressure on the Thermal Decomposition Kinetics, Chemical Reactivity and Phase Behavior of RDX", *Combust. Flame* 83, 174-184 (1991).
- (73) L.G. Harrison, "The Theory of Solid Phase Kinetics", in: C.H. Bamford and C.F.H. Tipper (eds), "Comprehensive Chemical Kinetics", Elsevier, New York 1969, Vol. 2, Ch. 5.
- (74) S.W. Benson, "The Foundations of Chemical Kinetics", McGraw-Hill, New York 1960, Ch. 4.
- (75) N.S. Cohen and C.F. Price, "Combustion of Nitramine Propellants", *J. Spacecr. Rockets* 12, 608-612 (1975).
- (76) N.S. Cohen, "Nitramine Propellant Research", AFOSR-TR-76-1163 [AD-A033034] (1976), Air Force Office of Scientific Research, Bolling AFB, DC, USA; *Chem. Abstr.* 86, 192059 (1977).
- (77) N.S. Cohen, "Nitramine Smokeless Propellant Research", NASA-CR-157150 (1977), Jet Propulsion Laboratory, Pasadena, CA, USA; *Chem. Abstr.* 89, 181931 (1978).
- (78) R.N. Kumar and L.D. Strand, "Theoretical Combustion Modeling Studies of Nitramine Propellants", *J. Spacecr. Rockets* 14, 427-433 (1977).
- (79) N.S. Cohen and L.D. Strand, "Analytical Model of High-Pressure Burning Rates in a Transient Environment", *AIAA J.* 18, 968-972 (1980).
- (80) N.S. Cohen, G.A. Lo, and J.C. Crowley, "Theoretical and Chemistry of HMX Combustion", *AIAA J.* 23, 276-282 (1985).
- (81) D.O. Woolery and J.E. Flanagan, "Burn Rate Characteristics of Solid Trinitromethyl Oxidizers with Inert and Energetic Binders", *27th JANNAF Combustion Meeting*, Warren AFB, WY, 5-9 November 1990, Chemical Propulsion Information Agency, Columbia, MD, USA.
- (82) M.A. Schroeder, R.A. Fifer, M.S. Miller, R.A. Pesce-Rodriguez, and G. Singh, "Condensed-Phase Processes During Solid Propellant Combustion. II. Chemical and Microscopic Examination of Conductively Quenched Samples of RDX, XM39, J-2, M30 and HMX Binder Compositions", *27th JANNAF Combustion Meeting*, Warren AFB, WY, 5-9 November 1990, Chemical Propulsion Information Agency, Columbia, MD, USA.

Acknowledgement

The authors gratefully acknowledge the financial support of the Air Force Office of Scientific Research/Directorate of Chemical and Atmospheric Sciences, Director Dr. D. Ball.

(Received June 21, 1992; Ms 38/92)

Accession For	
NTIS CRA&I	<input checked="" type="checkbox"/>
DTIC TAB	<input type="checkbox"/>
Unannounced	<input type="checkbox"/>
Justification	
By	
Distribution	
Date	
A-1, 20	